

## ENHANCEMENT OF VOLTAGE STABILITY WITH UNIFIED POWER FLOW CONTROLLER CONSIDERING LOADABILITY ANALYSIS

S.S. Yusuf\*<sup>1</sup>, P.U. Okorie<sup>2</sup>, A.S. Abubakar<sup>3</sup>, I.O. Onimisi<sup>4</sup> and F. Alhassan<sup>5</sup>

<sup>1,2,3,4</sup> Department of Electrical Engineering, Ahmadu Bello University,  
Zaria, Nigeria.

<sup>5</sup>Department of Electrical Engineering, Abdu Gusau Polytechnic, Talata-  
Mafara, Zamfara State, Nigeria.

*yusufssamuel@gmail.com*

### Article history:

Received Date:

2020-07-01

Accepted Date:

2020-09-12

Keywords:

Contingency,

Grey Wolf

Optimization,

Line Voltage

Stability Index,

Power System

Security, UPFC

**Abstract**— Voltage stability is an important issue in planning and operation of electric power system during both normal and under contingency conditions. This paper presents line voltage stability index (LVSI) for transmission lines voltage stability assessment and evaluation. The system stability under maximum loading and contingency conditions are analyzed using optimal power flow analysis. FACTS device is considered for a real-time control and a dynamic reactive power compensation of the system. Voltage source-based power injection model of unified power flow controller (UPFC) is used for the minimization of voltage deviation and losses on the network. Optimal location and sizing

of UPFC is carried out using grey wolf optimization (GWO) technique in order to identify an optimal location where the FACTS device will be installed. GWO is flexible, scalable and has the ability to strike the right balance between exploitation and exploration of the unknown search spaces and yields a favourable result at a very fast rate. The various conditions and scenarios used to test the efficacy of this model for system stability and security under contingency conditions are demonstrated on standard IEEE 14-bus test system. The simulation results have shown that UPFC device along with optimization technique increases the line transmittable power, controls the voltage magnitude at the buses as well as enhancing the stability and security of the power system.

## **I. Introduction**

Power system stability and security are important strategies in the system expansion and operation to meet or balance societal goals of energy demand in a way that, loads are completely supplied during both normal condition and under contingency at a least cost [1]. Voltage collapse and line overload are still the biggest threats to the transmission

system resulting from population growth and advancement in technology [2]. Various voltage indicators have been suggested for voltage stability analysis in [3]. These indices are important tools used to examine load stability and the influence of load model on the transmission line [4].

Transmission line loading capacity is characterized by a number of limits amongst which

are: thermal limit, steady-state stability limit, voltage-drop limit, voltage stability margin, voltage quality limit, and Joule losses [5-8]. Load characteristics are among the major driving forces of voltage instability and system collapse [9]. These problems and other factors result in power system insecurity [10, 11]. Constructing a new generating unit and transmission network to cater for the increase in demand will by far increase the system reliability and security, but these measures are constrained by rising cost of new facilities, political and environmental impacts. These challenges have strongly necessitated for the optimization and enhancement of the existing transmission lines to allow more power to be wheeled and delivered during both normal and contingency conditions without compromising the voltage stability [4, 9, 12, 13]. But with the innovation and incorporation of a compensating device like Flexible Alternative Current Transmission System (FACTS) devices, transmission line parameters such as voltage

magnitude, power flow, line loadability are enhanced [14], which will in turn satisfy or balance the demand growth being witnessed on the network. These devices allow power systems to be transmitted in a more sophisticated way and increase network's efficiency with less investment cost and little or no impact on the environment [14]. Amongst the numerous FACTS devices developed, unified power flow controller (UPFC) is the most versatile and widely used, because of its unique ability to simultaneously or independently controls all the three parameters of power flow: voltage magnitude, phase angle and line impedance [14-16]. This series-shunt compensator has the capacity to solve low voltage, oscillation damping, and relieve line congestions at a very fast rate. The performance of the device depends largely on the location and sizing on the network, as such a population-based meta-heuristic algorithm, grey wolf optimization technique is deployed for the optimal location and sizing of

the device, because of its scalability, flexibility, fast convergence and ability to attain a satisfactory result of the unknown search space at a very fast speed.

In this paper, optimal location of UPFC was carried out using GWO. Voltage stability indicator (LVSI) was used to estimate the loading margin of the network of each scenario. Installing FACTS device at appropriate location has a great influence on the performance of UPFC at enhancing the transmittable power, stability and security of power system by improving transmission capacity. The proposed approach is validated on IEEE-14 bus system and the solution is optimized by using GWO.

## II. Power System Security

Power System Security is defined as the ability of a system to survive short-circuits or unexpected failures and still continue to operate without interruption of supply to consumers [17, 18]. The continuous sequences of voltage level variability will results in

voltage collapse and subsequently in total or partial blackout[19]. Voltage instability is a major concern for secure operation of many power stations [4, 9]. The security issues that restrict the power transmission line capacity are the steady-state stability, frequency collapse, transient stability, voltage collapse, sub-synchronous resonance etc. [5].

### A. Line voltage stability index (LVSI)

Line voltage stability index is a voltage indicator used to assess and evaluate the voltage stability and loading margin of a network [4]. Most previous indices reflect the likelihood but not the severity, while LVSI captures both likelihood and severity [4]. This index is formulated from a voltage quadratic equation based upon  $ABCD$  transmission line parameters. The sending end voltage/current of a line can be related to receiving end voltage/current using  $ABCD$  parameter as shown in (1):

$$\begin{bmatrix} V_S \\ I_S \end{bmatrix} = \begin{bmatrix} A & B \\ C & D \end{bmatrix} \begin{bmatrix} V_R \\ I_R \end{bmatrix} \quad (1)$$

The terms **A**, **B**, **C** and **D** are known as the transmission line parameters related to two-port network shown in Table 1.

Table1: Relation of transmission line and two-port network

|                                     |  |
|-------------------------------------|--|
| $A = \left(1 + \frac{ZY}{2}\right)$ | Open circuit<br>reverse voltage<br>transfer ratio  |
| $B = Z$                             | Short circuit<br>reverse transfer<br>impedance     |
| $C = \left(1 + \frac{ZY}{4}\right)$ | Open circuit<br>reverse transfer<br>admittance     |
| $D = A$                             | Short circuit<br>reverse current<br>transfer ratio |

where,  $Z$  and  $Y$  are the transmission line impedance and line charging admittance respectively[4].

The active power at the receiving end is mathematical model in equation (2):

$$P_R = \frac{V_S V_R \cos(\beta - \delta)}{B} - \frac{A V_R^2 \cos(\beta - \delta)}{B} \quad (2)$$

This can be written in quadratic form of the voltage equation as thus:

$$V_R^2 = \frac{V_S V_R \cos(\beta - \delta)}{A \cos(\beta - \alpha)} - \frac{P_R B}{A \cos(\beta - \alpha)} \quad (3)$$

The Line Voltage Stability Index is hereby formed in equation (4):

$$LVSI_j = \frac{2V_{Rj} A_j \cos(\beta_j - \alpha_j)}{V_{Sj} \cos(\beta_j - \delta_{SRj})} \quad (4)$$

From equation (4), it can be deduced that when the value of the proposed index is 2 it denotes no-load condition, which signify a wide voltage stability margin. As the loading of the network increases, the value of the index (LVSI<sub>j</sub>) decreases which shows a reduction in voltage stability margin. At maximum loading point, the index value of the line reaches 1, which indicates critical state of the line.

## **B. Modelling of unified power flow controller**

This device comprises of series and shunt static converters, as shown in Figure 1, a dc storage capacitor provides a DC links between the two converters. The series inverter is connected to the transmission line through a (boosting) transformer and the

shunt inverter is connected together to a local bus through a shunt-connected exciting transformer. The inverted (shunt) serves as both generator and absorber of active and reactive power. The series (converter 2) is utilized to produce voltage source at the fundamental frequency with variable amplitude ( $0 \leq V_T \leq V_{Tmax}$ ) and phase angle ( $0 \leq Q_T \leq 2\pi$ ), this is added to the AC transmission line by the series connected boosting transformer. UPFC is a device that allows two ways flow of power involving the shunt output terminals of static compensator (STATCOM) and series output terminals of static synchronous series compensator (SSSC). It also offers the role of independent advance static VAR compensator by providing power compensation for the transmission line. This voltage source is capable of generating or absorbing internally all the needed reactive power by the different types of controls applied and transfers active power at its DC terminal to ensure a secure and stable

system. Figure 1 shows a typical operating principle of UPFC.

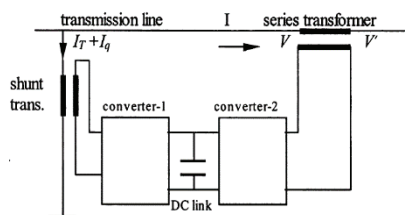


Figure 1: The Operating principle of UPFC [15, 20]

The real power and reactive power injection at the bus-*i* with the system loading ( $\lambda$ ) is given by (5) and (6):

$$P_i = P_{gi} - P_{di}^0(1 + \lambda) = \sum_{j \in N_b} P_{ij} \quad (5)$$

$$Q_i = Q_{gi} - Q_{di}^0(1 + \lambda) = \sum_{j \in N_b} Q_{ij} \quad (6)$$

Detailed of the modelling equations are shown in [15].

### C. Grey Wolf Optimization Technique

GWO is a population-based meta-heuristic algorithm developed by [21] based on the leadership hierarchy and hunting behaviour of a grey wolf (*Canis lupus*). Wolves are social animal of four categories in the hierarchical order of alpha ( $\alpha$ ), beta ( $\beta$ ), delta ( $\delta$ ), and omega ( $\omega$ ) [22]. There are three phases of

hunting; tracking the prey, encircling the prey and attacking towards the prey. Hunting in the pack is carried out by alpha ( $\alpha$ ), beta ( $\beta$ ) and delta ( $\delta$ ). Alpha are the leaders (male and a female) in a pack and also determines the fittest solution due to its best searching knowledge, while the beta ( $\beta$ ) is a follower with second best solution and delta ( $\delta$ ) gives the third best solution, while gamma is the other candidate solutions, babysitter in

the pack and least level in the hierarchy [23]. The algorithm has proven to have a wider exploitation and exploration to solve non-linear engineering optimization problems and attained a satisfactory result of the unknown search space at a very fast rate when compared with other algorithms [21]. Figure 2 shows position updating mechanism of search agents.

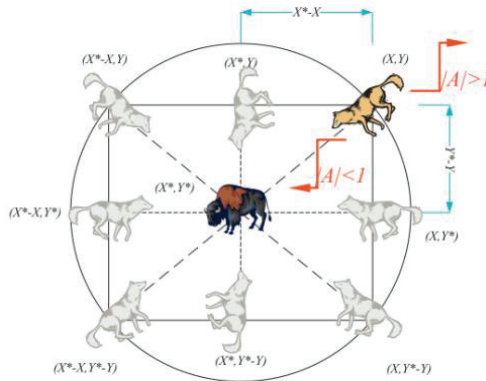


Figure 2: Position updating mechanism of search agents [21]

The hunting mechanisms of grey wolves are mathematical model as follows:

(a) Encircling prey

The first stage in hunting is to circle-shaped the region of the prey. This behaviour is

mathematically model in equations (7) and (8):

$$\vec{K} = \left| \vec{A} \cdot \vec{W}_p(t) - \vec{W}(t_i) \right| \quad (7)$$

$$\vec{W}(t_{i+1}) = \vec{W}_p(t_i) - \vec{S} \cdot \vec{K} \quad (8)$$

where:

$\vec{S}$  and  $\vec{A}$  are coefficient vectors;  $\vec{W}_p$  is the position vector of the prey;  $\vec{W}$  denote grey wolf vector position;  $t_i$  indicates the current iteration.

The vectors  $\vec{S}$  and  $\vec{A}$  are calculated using (9):

$$\vec{S} = 2\vec{a}\vec{r} - \vec{a} \text{ and } \vec{A} = 2\vec{r}_2 \quad (9)$$

### (b) Hunting

This is a process of moving towards the prey using the information acquired in equations (7) and (8) respectively. The alpha, beta and delta positions are model in equations (10) and (11):

$$\vec{K}_\alpha = |\vec{A}_1 \cdot \vec{W}_\alpha - \vec{W}|, \vec{K}_\beta = |\vec{A}_2 \cdot \vec{W}_\beta - \vec{W}|, \vec{K}_\delta = |\vec{A}_3 \cdot \vec{W}_\delta - \vec{W}| \quad (10)$$

$$\vec{W}_1 = |\vec{W}_\alpha - \vec{S}_1 \cdot (\vec{K}_\alpha)|, \vec{W}_2 = |\vec{W}_\beta - \vec{S}_2 \cdot (\vec{K}_\beta)|, \vec{W}_3 = |\vec{W}_\delta - \vec{S}_3 \cdot (\vec{K}_\delta)| \quad (11)$$

The best solution is obtained by taking the average of (11) as follows (12):

$$\vec{W}_{(t_i+1)} = \frac{\vec{W}_1 + \vec{W}_2 + \vec{W}_3}{3} \quad (12)$$

### (c) Attacking prey (exploitation)

The grey wolves finished the hunting by attacking the prey when it stops moving. If  $[\vec{S}] > 1$ , then the best candidate solutions is diverge from the prey to find a fittest prey and when  $[\vec{S}] < 1$  candidate solutions converge and then force the wolves to go after the prey [24]. The GWO algorithm terminates by the satisfaction of an end criterion.

## III. Optimal Power Flow Problem Formulation

The objective of this paper is to enhance voltage stability of an interconnected system by improving the power carrying capacity of the transmission line.

### A. Minimization of Real Power Loss

$$\text{Minimize } P_{loss}(x, y) \quad (13)$$

Subject to:

$$h(x, y) = 0, \quad g(x, y) \leq 0 \quad (14)$$

$$\min P_{loss} = \sum_{k=1}^{N_l} [G_k (V_i^2 + V_j^2 - 2V_i V_j \cos \theta_{ij})] \quad (15)$$

where:

$h$  is the equality constraint representing active and reactive



power balance equation;  $g$  is the system operating constraints; ( $P_{loss}$ ) is active power loss;  $g_k$  is the conductance of branch  $k$ ;  $V_i$  and  $V_j$  are the magnitude of voltage at sending end and receiving end buses respectively;  $\theta_{ij}$  is the phase angle difference between  $i^{th}$  and  $j^{th}$  bus.

### B. Voltage Deviation (VD)

This objective function is aimed at minimizing the voltage deviation at all load buses and improving the voltage profile. This is expressed mathematically in (16):

$$F_{VD} = \min \left( \sum_{k=1}^N |V_i - V_j^{ref}|^2 \right) \quad (16)$$

where:  $V_i$  is voltage at bus  $i$  and  $V_j^{ref}$  reference voltage limit at bus  $j$ , taking as 1.0 p.u.

### C. The Equality Constraints

The Active and reactive power equality constraints are given in (17) and (18):

$$0 = P_{Gi} - P_{Di} - V_{Gi} \sum_{j \in N_i}^{Nb} V_j (G_{ij} \cos \theta_{ij} + B_{ij} \sin \theta_{ij}) \quad (17)$$

$i \in N_b$

$$0 = Q_{Gi} - Q_{Di} - V_{Gi} \sum_{j \in N_i}^{Nb} V_j (G_{ij} \sin \theta_{ij} + B_{ij} \cos \theta_{ij}) \quad (18)$$

$i \in N_b$

where:  $N_b$  is the total number of buses;  $Q_{Gi}$  is the generation of reactive power;  $P_{Gi}$  is the total real power generation;  $P_{Di}$  is the total power demand;  $Q_{Di}$  is the reactive power demand;  $G_{ij}$  and  $B_{ij}$  denote conductance and susceptance between  $i^{th}$  and  $j^{th}$  bus respectively.

### D. Operational (Inequality) Constraints

The voltage, reactive power and active power limit of the generator is given by:

$$V_{Gi}^{\min} \leq V_{Gi} \leq V_{Gi}^{\max} \quad i \in N_g \quad (19)$$

$$Q_{Gi}^{\min} \leq Q_{Gi} \leq Q_{Gi}^{\max} \quad i \in N_g \quad (20)$$

$$P_{Gi}^{\min} \leq P_{Gi} \leq P_{Gi}^{\max} \quad k = 1, \dots, N_g \quad (21)$$

Transformer tap-setting lower and upper limits are expressed by the constraints in (22) and (23):

$$T_i^{\min} \leq T_i \leq T_i^{\max} \quad i \in N_T \quad (22)$$

$$V_i^{\min} \leq V_i \leq V_i^{\max} \quad k = 1 \in N_L \quad (23)$$

#### IV. Results and Discussion

The IEEE 14-Bus network consisting of twenty transmission lines, five generators, three tap-changing transformers and one shunt compensator is used for these analyses. In a steady-state stability analysis, IEEE 14-bus network is regarded as the most insecure bus because it has the lowest voltage magnitude when compared with other IEEE standard buses. These analyses are divided into two scenarios: loadability analysis at maximum loading and loadability analysis during contingency conditions with or without UPFC.

##### A. Maximum Loadability Limit without Contingency

In order to determine the performance of the FACTS device, GWO algorithm was run to determine the position of the device on the network under 49.95% of load increase at computational time ( $t$ ) of 120s. Table 2 shows the loading value of IEEE 14-bus under increase

percentage load demand index of 49.95% at all the load buses, real power loss of 62.4711MW was obtained and after optimal placement of UPFC, it reduces to 30.8996MW representing 50.54% loss reduction with installation of 79.5000MVar size of UPFC at bus 5. The voltage profile at the heavy loading of 49.95% is shown in Figure 3; violation of voltage nominal tolerance of  $\pm 5\%$  is recorded at Buses 9, 10 and most especially Bus 14, due to the cascading effects. The other load buses like 4, 5, 6, 7, 12 and 13 were very close to their lower boundaries, which mean any further increase in the load demand will result in voltage collapse. It is therefore mean 49.95% loading is the optimum loadability of IEEE 14-bus system under the operating range of 0.95-1.05p.u. It is also observed from the Figure 3, that bus 4 has the maximum voltage deviation as obtained by GWO algorithm. It is also inferred from Figure 3 that any further increase in the demand load will result in the unstable of the entire system, because buses 10

and 14 have reached their lower limits of voltage amplitude. With an optimal location of UPFC using GWO at Bus 5, it shows voltage stability enhancement by increasing the

voltage stability margin of the system to enable more power to be transmitted over the existing network.

Table 2: Maximum Loading and Location of UPFC using GWO with and without UPFC

| Maximum Loading (%) | Losses Without UPFC (MW) | Rating of UPFC (MVar) | Losses With UPFC (MW) | UPFC Location | % Power Loss Reduction |
|---------------------|--------------------------|-----------------------|-----------------------|---------------|------------------------|
| 49.95               | 62.4711                  | 79.50                 | 30.8996               | 5             | 50.54                  |

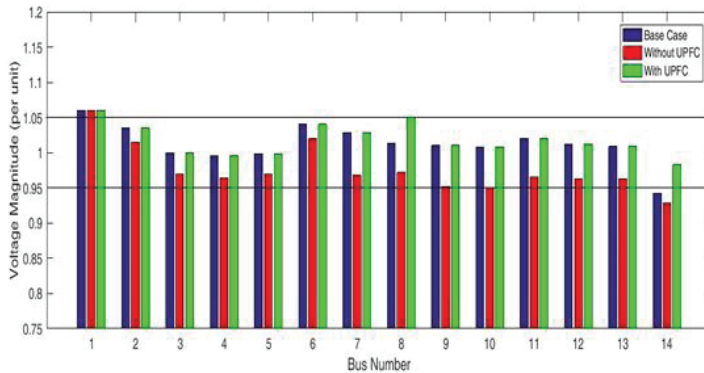


Figure 3: Voltage profile results under maximum loading condition

### B. Heavy Reactive Loading (52.75%) at Single Bus with Single Generator Outage

The bus 13 which is one of the most sensitive buses is increased to reach the maximum reactive power flow (a level of voltage collapse) at 52.75%, and bus 2 (generator bus) is made out of

service. The optimal location and sizing of UPFC device is determined based on the GWO algorithm by taking into consideration all contingencies for the improvement of network loadability, security and maintenance of voltage stability. The result of the LVSI before and after heavy loading is

computed and tabulated in Table 3. The index value is close to 2, for no-load condition and decreases from 2 to 1 with increase in transmission line loading. From Table 3, it is observed that before loading, all voltages were within voltage tolerance, but after heavy reactive power loading at one bus and a single generator outage, the voltage magnitude decreases. The power flow result is given in Figure 4, the highest voltage dip occurs at Bus-13 (0.9670), this was due to the loss of generation (reactive power) that should have come from Bus 2 that was made out of service and this shows the high negative effect of generator outage on the voltage magnitude. It is also observed from the Figure 4, that the voltage magnitude at buses 4, 5, 7, 9, 10, 12 and 14 drastically decreases due to their nearer connections to the critical lines and the generator outage that results in the lack of generation (reactive power) to support the system. But in the presence of UPFC with reactive power setting of -87.16MVar optimally placed by GWO at bus 14, it is

observed that voltage improvement is noticed in all the buses. It is also evident that UPFC has also salvaged the voltage violations and increase voltage magnitude at buses 4, 5, 7, 9, 11, 13 and 14. It is identified that lack of generation at Bus 2, increases the losses at line 2 to 46MVar from the base case of 16.4MVar with subsequent cascading effect on Buses 4 and 5 due to their nearer connection to the critical lines. Likewise, it is noticed from the results, that lack of generation at bus 2 was compensated by the slack generator at bus 1. Also at Bus 13 where the highest reactive power loss occurs due to the heavy loading and loss of generation, a reactive power loss of 144.6MVar was recorded when compared with the base case. The effect of Bus 13 was also visible on the nearer lines like 10 and 12 due to the cascading failure effect. UPFC size -87.16MVar was optimally placed on Bus14 to inject more reactive power to stabilize the system from voltage collapse. Line 2 with 44MVar loss reduced to 8.4MVar (89.91%

reduction) and loss of 144.6MVar at line 13 was subsequent reduced to 6.32Mvar (95.85% reduction) through the injection of more reactive power to the system by the UPFC.

These have shown the ability of UPFC at enhancing power flow in transmission line, improving bus voltage and power losses reduction.

Table 3: Voltage Stability index for IEEE 14-bus system under Heavy Reactive Loading of Single bus with single Generator Outage

| Bus No | Loading Value (MVar) | LVSI Before Heavy Loading | LVSI After Heavy Loading |
|--------|----------------------|---------------------------|--------------------------|
| 4      | 46.6191              | 1.8167                    | 1.0082                   |
| 5      | 55.8453              | 1.7100                    | 1.0053                   |
| 7      | 14.6969              | 1.9145                    | 1.0414                   |
| 9      | 27.2397              | 1.7895                    | 1.0275                   |
| 10     | 75.4215              | 1.7605                    | 1.0258                   |
| 12     | 42.8123              | 1.8765                    | 1.0336                   |
| 13     | 102.0630             | 1.8146                    | 1.0317                   |
| 14     | 62.5483              | 1.7161                    | 1.0140                   |

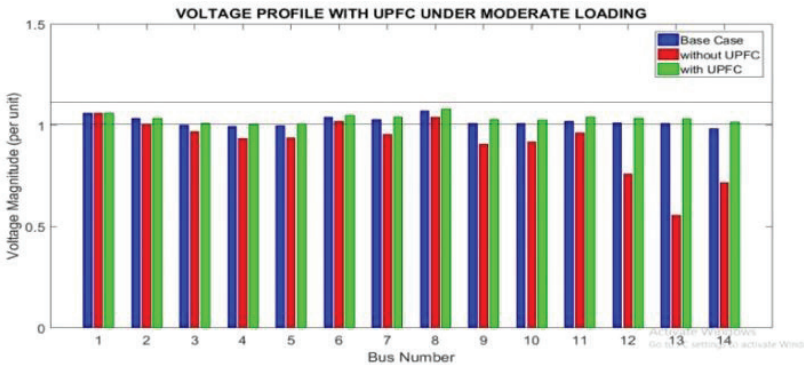


Figure 4: Heavy Reactive Loading at single bus with single Generator Outage

### C. Heavy Real Load of Single Bus with Single (N-1) Line Outage

The 6<sup>th</sup> line which is a critical line is made out of service and Bus 9 real power is raised to

55.80% a point of voltage collapse. Then the optimal location and sizing of UPFC device was determined based on the GWO algorithm by taking into consideration all

contingencies for transmission line capacity improvement and to maintain voltage stability. The result of the LVSI before and after heavy loading is computed and tabulated in Table 4. The index value decreases from 2 to 1 with increase in transmission line loading and single line outage. The power flow result for all the load buses are presented in Figure 5. Based on the result obtained, buses 9 (0.7166) and 10 (0.7492) have the highest voltage sags. But with the installation of the UPFC of size -92.51MVar at bus 5, the voltage sags were adequately compensated through the injection of sufficient reactive power to maintain a stable

network by keeping all the voltage buses within the acceptable limit. The load flow analysis diverged instead of converging with further increase in the real power load demand in Bus 9 beyond 55.80%. The critical voltage occurs at bus 9 (0.7166p.u). But with the optimal installation of UPFC at bus 5 the violated voltages were normalized as shown in Figure 5. It is evident that, UPFC has the capability to control all the three parameters of power flow: voltage magnitude, phase angle and line impedance and to completely delivered power during both normal and under contingency conditions at the least cost.

Table 4: Voltage Stability index for IEEE 14-bus system under Heavy Real of Single bus with single Line Outage

| <b>Bus No</b> | <b>Loading Value (MW)</b> | <b>LVSI Before Heavy Loading</b> | <b>LVSI After Heavy Loading</b> |
|---------------|---------------------------|----------------------------------|---------------------------------|
| 4             | 79.7419                   | 1.9295                           | 1.0597                          |
| 5             | 62.5689                   | 1.9451                           | 1.0705                          |
| 7             | 38.7763                   | 1.9902                           | 1.0567                          |
| 9             | 40.7189                   | 1.9502                           | 1.0076                          |
| 10            | 43.5425                   | 1.9475                           | 1.0392                          |
| 13            | 128.7754                  | 1.9568                           | 1.0971                          |
| 14            | 50.1452                   | 1.8979                           | 1.0401                          |

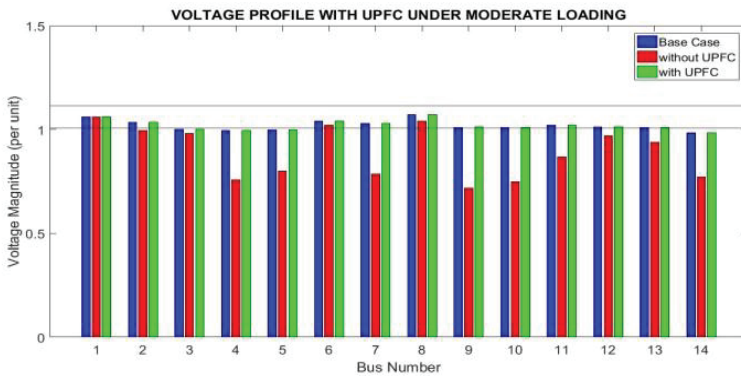


Figure 5: Voltage stability analysis for heavy active loading of single bus with  $(N-1)$  Outage

## V. Conclusion And Future Scope

This paper presents Grey Wolf Optimization (GWO) technique for system security enhancement and maintenance of voltage stability through the optimal installation of UPFC. It is evident that UPFC enhances the load capacity of the existing transmission line to accommodate more power through it and also to wheel and delivered power to the users at both normal and contingency conditions. The algorithm used has proven to have a wider exploitation and exploration of the unknown search space and in obtaining optimal or near-optimal location of UPFC on the network. The efficacy and the robustness of this technique are

demonstrated by using Newton-Raphson load flow to analyze the voltage stability improvement under maximum loadability and during contingencies before and after optimal placement of the UPFC. Finally, it can be concluded that more power can be transmitted to meet ever-growing demand over an existing network without compromising the voltage stability by using the cheaper plan proposed in this methodology.

This work can further be extended by using the combination of series and shunt FACTS devices like GUPFC and IPFC that can handle multiple lines simultaneously.

## VI. References

- [1] H. Hakim, "Application of Pattern Recognition in Transient Security Assessment," *Electric Power Components and Systems*, vol. 20, pp. 1-15, 1992.
- [2] M. J. Vahid-Pakdel, H. Seyedi, and B. Mohammadi-Ivatloo, "Enhancement of power system voltage stability in multi-carrier energy systems," *International Journal of Electrical Power & Energy Systems*, vol. 99, pp. 344-354, 2018/07/01/ 2018.
- [3] J. Modarresi, E. Gholipour, and A. Khodabakhshian, "A comprehensive review of the voltage stability indices," *Renewable and Sustainable Energy Reviews*, vol. 63, pp. 1-12, 2016/09/01/ 2016.
- [4] S. Ratra, R. Tiwari, and K. R. Niazi, "Voltage stability assessment in power systems using line voltage stability index," *Computers & Electrical Engineering*, 2018/01/05/ 2018.
- [5] I. Khan, M. A. Mallick, M. Rafi, and M. S. Mirza, "Optimal placement of FACTS controller scheme for enhancement of power system security in Indian scenario," *Journal of Electrical Systems and Information Technology* vol. 2, pp. 161-171, 2015.
- [6] N. H. Patel, V. Thakkar, and H. N. Raval, "Contingency Analysis in Power System and Remedial Actions," *IJSRD - International Journal for Scientific Research & Development*, vol. 3, pp. 821-827, 2015.
- [7] C. J. Nnonye, T. C. Madueme, and B. Anyaka, "Power System Contingency Analysis: A Study of Nigeria's 330KV Transmission Grid," in *Proceedings of the 4 th Electrical Engineering National Conference on Energy sources for power generation*, 2013, pp. 21-23.
- [8] S. Quaia, "Critical analysis of line loadability constraints," *International Transactions on Electrical Energy Systems*, p. e2552, 2018.
- [9] M. V. Suganyadevi and C. K. Babulalb, "Estimating of Loadability Margin of a Power System by comparing Voltage Stability Indices," *International Conference on "Control, Automation, Communication and Energy Conservation*, pp. 1-5, 2009.
- [10] J. J. Paserba, "How FACTS Controllers Benefit AC Transmission Systems," *IEEE Press*, 2003.
- [11] T. G. Manohar and R. S. Reddy, "Literature Review on Voltage stability phenomenon and Importance of FACTS Controllers In power system Environment," *Global Journal of Researches in Engineering Electrical and Electronics Engineering*, vol. 12, pp. 24-29, 2012.
- [12] S. Raj and B. Bhattacharyya, "Optimal placement of TCSC and SVC for reactive power planning using Grey wolf optimization algorithm," *Swarm and Evolutionary Computation BASE DATA*, pp. 1-29, 2017.
- [13] A. O. Emmanuel, K. O. Ignatius, and E. A. Abel, "Enhancement of Power System Transient Stability - A Review," *IOSR Journal of Electrical and Electronics Engineering (IOSR-JEEE)*, vol. 12, pp. 32-36, 2017.
- [14] S. Ravindra, C. V. Suresh, S. Sivanagaraju, and V. C. Reddy,



- "Power System Security Enhancement with Unified Power Flow Controller under Multi-event Contingency Conditions," *Ain Shams Engineering Journal*, pp. 1-10, 2015.
- [15] K. S. Verma, S. N. Singh, and H. O. Gupta, "Location of unified power flow controller for congestion management," *Electric Power Systems Research*, vol. 58, pp. 89-96, 2001/06/21/ 2001.
- [16] S. S. Yusuf, J. Boyi, O. P. Ubeh, A. A. Saidu, and M. I. Onimisi, "Transmission Line Capacity Enhancement with Unified Power Flow Controller Considering Loadability Analysis," *ELEKTRIKA-Journal of Electrical Engineering*, vol. 18, pp. 8-12, 2019.
- [17] T. A. Kumar and I. A. Chidembaram, "Power System Security Enhancement using FACTS devices in a Power System Network with Voltage Dependent Loads and ZIP Loads," *International Journal of Computer Applications*, vol. 45, pp. 26-37, 2012.
- [18] D. S. Kirschen, "Power System Security," *Power Engineering Journal* pp. 241-248, 2002.
- [19] C. H. Rambabu, Y. P. Obulesu, and C. H. Saibabu, "Improvement of Voltage Profile and Reduce Power System Losses by using Multi Type Facts Devices," *International Journal of Computer Applications*, vol. 13, pp. 37-41, 2011.
- [20] X. P. Zhang, C. Rehtanz, and B. Pal, *Flexible AC Transmission Systems: Modelling and Control*. Heidelberg New York Dordrecht London: Springer, 2012.
- [21] S. Mirjalili, S. Mohammad, and A. Lewis, "Advances in Engineering Software Grey Wolf Optimizer," *Advances in Engineering Software*, vol. 69, pp. 46-61, 2014.
- [22] L. D. Mech, "Alpha status, dominance, and division of labor in wolf packs," *Can. J. Zool*, vol. 77, pp. 1196-1203, 1999.
- [23] D. P. Ladumor, R. H. Bhesdadiya, I. N. Trivedi, and P. Jangir, "Optimal Power Flow with Shunt Flexible AC Transmission System (FACTS) Device Using Grey Wolf Optimizer," *3rd International Conference on Advances in Electrical, Information Communication and Bio-Informatics (AEEICB17)*, 2017.
- [24] R. K. Mallick and N. Nahak, "Grey Wolves-Based Optimization Technique for tuning damping controller parameters of unified power flow controller," *International Conference on Electrical, Electronics, and Optimization Techniques (ICEEOT)* pp. 1458-1463, 2016.

